Caspase activation and neuroprotection in caspase-3-deficient mice after *in vivo* cerebral ischemia and *in vitro* oxygen glucose deprivation

Dean A. Le*[†], Yongqin Wu*[†], Zhihong Huang*, Kohji Matsushita*, Nikolaus Plesnila*, Jean C. Augustinack[‡], Bradley T. Hyman[‡], Junying Yuan[§], Keisuke Kuida[¶], Richard A. Flavell[∥], and Michael A. Moskowitz*,**

*Stroke and Neurovascular Regulation Laboratory and [‡]Alzheimer's Disease Research Unit, Massachusetts General Hospital, [§]Department of Cell Biology, Harvard Medical School, Boston, MA 02114; [¶]Vertex Pharmaceuticals, Inc., Cambridge, MA 02139; and [∥]Section of Immunology and Howard Hughes Medical Institute, Yale University School of Medicine, New Haven, CT 06510

Caspase-3 is a major cell death effector protease in the adult and neonatal nervous system. We found a greater number and higher density of cells in the cortex of caspase-3$^{-/-}$ adult mice, consistent with a defect in developmental cell death. Caspase-3$^{-/-}$ mice were also more resistant to ischemic stress both *in vivo* and *in vitro*. After 2 h of ischemia and 48 h of reperfusion, cortical infarct volume was reduced by 55%, and the density of terminal deoxynucleotidyl-transferase-mediated dUTP nick end labeling-positive cells was decreased by 36% compared with wild type. When subjected to oxygen-glucose deprivation (2 h), cortical neurons cultured from mice deficient in caspase-3 expression were also more resistant to cell death by 59%. Mutant brains showed caspase-specific poly-(ADP-ribose) polymerase cleavage product (85-kDa fragment) *in vivo* and *in vitro*, suggesting redundant mechanisms and persistence of caspase-mediated cell death. In the present study, we found that caspase-8 mediated poly(ADP-ribose) polymerase cleavage in caspase-3$^{-/-}$ neurons *in vivo* and *in vitro*. In addition, mutant neurons showed no evidence of compensatory activation by caspase-6 or caspase-7 after ischemia. Taken together, these data extend the pharmacological evidence supporting an important role for caspase-3 and caspase-8 as cell death mediators in mammalian cortex and indicate the potential advantages of targeting more than a single caspase family member to treat ischemic cell injury.

Caspases play an essential role during apoptotic cell death (1, 2). Among 14 distinct caspases, caspase-3 is crucial during neuronal development and under pathological conditions including cerebral ischemia (3–5). Caspase-3 is also the most abundant cysteine aspartase expressed in adult rodent brain and caspase-3-like enzyme activity and activated caspase-3 subunits are detected in ischemic tissues by immunoblotting and immunohistochemistry (6, 7). Treatment with peptide-based caspase inhibitors protects brain from mild ischemic injury and improves neurological deficits (8–10). We extend the findings above by studying ischemic mechanisms in caspase-3$^{-/-}$ brain *in vivo* and *in vitro*.

Unlike the caspase-3$^{-/-}$ mice generated on a 129/Sv background, caspase-3$^{-/-}$ mice bred on a C57BL/6 background survive until adulthood (11–13). These mice are congenitally deaf because of a defect in the development of the organ of Corti (14) but are otherwise phenotypically normal. By using these mice, we addressed whether selective caspase-3 inhibition or pancaspase blockade might be more therapeutically useful in ischemic injury. First, we asked whether ischemic injury was attenuated after caspase-3 deletion *in vivo* by using a distal middle cerebral artery occlusion model. Second, we addressed intrinsic cellular mechanisms related to caspase-3 deletion by studying cell death in enriched neuronal cultures subjected to oxygen-glucose deprivation (OGD). Because of persistent terminal deoxynucleotidyltransferase-mediated dUTP nick end labeling (TUNEL) staining and cleaved poly(ADP-ribose) polym-erase (PARP; 85 kDa) in both caspase-3$^{-/-}$-cultured neurons and within the ischemic brains of mutant mice, we searched for redundant activation of caspase(s) and explored the role of other caspases including caspase-6, -7, and -8 in the absence of caspase-3.

Materials and Methods

Caspase-3$^{-/-}$ Mice. Animal care and experimental protocols complied with National Institutes of Health *Guide for the Care and Use of Laboratory Animals* (15). Generation and characterization of caspase-3$^{-/-}$ mice and their WT littermates were described (11). Caspase-3$^{-/-}$ mice were backcrossed to C57BL/6 mice for at least five generations and resulting offspring were subsequently bred to generate homozygous offspring that survive more than 6 months. Genotyping of the offspring was performed by PCR of tail DNA extracts and by Western blot of caspase-3 proforms.

Ischemia Model. Transient occlusion of the middle cerebral artery (MCA) was performed as described (16). Adult caspase-3$^{-/-}$ and WT littermate mice (6–8 weeks) were anesthetized and rectal temperature was maintained at ≈37°C. An incision was made between the right ear and orbit, followed by a 1-mm craniotomy. The MCA was ligated distal to the lenticulostriate branches with 10-0 monofilament nylon. Regional cerebral blood flow was monitored by Laser Doppler (PF2B, Järfälla, Sweden) and was reduced from 100% to <35% after middle cerebral artery occlusion (MCAO) in all animals. Two hours after ischemia, the MCA ligature was removed and the animals were killed at 24 and 48 h after reperfusion. Randomly selected animals (*n* = 4 per group) were monitored for physiological parameters including blood pressure (mmHg), heart rate (beats per min), rectal temperature, and arterial blood gases as described (8, 17).

Determination of Infarct Size. Caspase-3$^{-/-}$ (*n* = 7) and WT littermate (*n* = 9) mice were killed 48 h after reperfusion. Ten-micrometer coronal brain sections were cut on a cryostat (Microm, HM505 E, Walldorf, Germany). Five sections from anterior striatum to posterior hippocampus were selected, taken at equally spaced 1.5-mm intervals. Infarct size was determined on hematoxylin/eosin-stained sections as described (17, 18).

Murine Neuronal Cell Cultures and OGD. Primary mouse neurons were prepared from E14–E15 embryos as described (19, 20). Because of the scarcity of caspase-3$^{-/-}$ mice, we impregnated caspase-3$^{-/+}$ adult female mice with caspase-3$^{-/+}$ adult males. Cortical cells from individual embryos were plated onto 48-well Falcon plates or 25-mm dishes at a density of 200,000 per cm^2. Cultures on *in vitro* day 9–10 from WT and caspase-3$^{-/-}$ embryos were selected for *in vitro* studies. When specified, neuronal cultures were also obtained from embryos of WT C57BL6 pregnant mice (Charles River Breeding Laboratories). OGD was performed in murine neocortical cell cultures and cell death was quantified by using Hoechst staining for condensed or fragmented nuclei as reported (20).

TUNEL. TUNEL staining was performed as described (21). For *in vitro* studies with TUNEL labeling in neuronal cell cultures, the chromogen diaminobenzidine was used (DeadEnd kit, Promega). For *in vivo* studies, the *in situ* Cell Death Detection kit was used (Roche Molecular Biochemicals) with either diaminobenzidine or streptavidin-conjugated Bodipy as chromogen.

RT-PCR. Total RNA was isolated from normal or ischemic and contralateral cortex ($n = 4$ per group) reperfused for 24 h and subjected to RT-PCR by using the mouse primers for caspase-8 as described (21).

Immunohistochemistry. Caspase-3$^{-/-}$ and WT mice ($n = 5$ per group) were killed 24 h after reperfusion. Immunohistochemical staining was performed as described (21) with few modifications. Primary antibodies (1:1,000, rabbit polyclonal antisera unless specified otherwise) were MF467 (against caspase-3 p33), SK441 (caspase-8 p55), SK440 (caspase-8 p18), and G734 (PARP p85; 1:100, mouse mAb; Promega). Appropriate biotinylated goat anti-rabbit or anti-mouse IgG (1:300; Vector Laboratories) were used as a secondary antibody. In control brain sections, incubation of primary antibodies was skipped. Double staining of cells containing a caspase plus NeuN (a neuronal marker) or TUNEL was performed. Brain sections were incubated with streptavidin-conjugated Cy3 (1:1,000, Jackson Immuno-Research) for 30 min. The sections were then incubated with NeuN (mAb, 1:300, Chemicon) for 1 h then with Bodipy FL-conjugated anti-mouse IgG (1:200, Molecular Probes). The sections were visualized on a Leica DMRB/Bio-Rad MRC 1024 confocal microscope. For Bodipy FL, excitation and emission filters were 488 and 522 nm, respectively. For Cy3, excitation and emission filters were 568 and 585 nm, respectively.

Stereology. Total neuron counts (NeuN-positive cells; $n = 6$ animals per group) were performed by using standard stereological optical dissector methods (22) on 10-μm coronal brain sections stained with cresyl violet. Data were recorded by using the Bioquant Image Analysis System (Nashville, TN). Four sections were selected from anterior striatum, posterior striatum, anterior hippocampus, and posterior hippocampus levels of the left hemisphere. The boundaries were the cingulate gyrus dorsally and medially, and the medial entorhinal cortex ventrally. The number of neurons was estimated by using ≈200 optical dissectors (50 × 50 μm per dissector with extended exclusion lines). Neuronal density was calculated by dividing the sum of the neurons counted by the product of counting frame area and the section thickness, and total neurons was estimated by multiplying the neuronal density by the reference volume (22).

Western Blotting. Brain homogenates of animals subjected to MCAO and lysates of neuronal cultures were obtained as described (20, 21). Liver homogenates from caspase-3$^{-/-}$ mice and WT mice injected with anti-Fas antibody (Jo-2) were obtained as described (13). Equal amounts of protein (20–30 μg
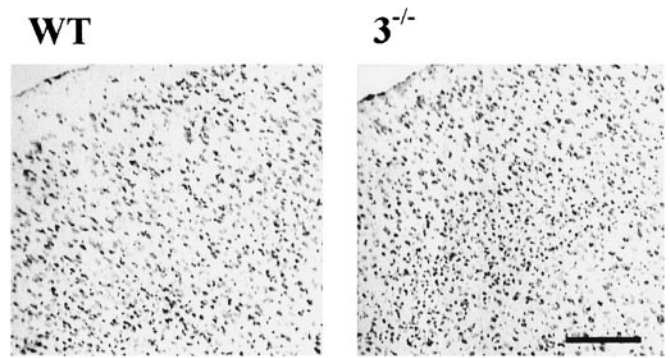
Fig. 1. Low-power photomicrograph (cresyl violet stain) showing hypercellularity in caspase-3$^{-/-}$ frontal cortex in comparison with WT littermates. (Bar = 100 μm.)

per lane) were separated by SDS/PAGE and then transferred to Immobilon-P membranes (Millipore). Probing of membranes with appropriate antibodies and detection of proteins of interest were according to procedures described (20, 21). Unless specified otherwise, immunoblots of two to three independent experiments were obtained in all studies.

PARP Cleavage Assay. Tissues from cortex of WT and caspase-3$^{-/-}$ mice ($n = 2$ animals per group) were homogenized by sonication (100 Sonic Dismembrator, Fisher Scientific) at 4°C in a buffer (1:4 wt/vol) containing 20 mM Hepes (pH 7.4), 2 mM EDTA, 0.1% 3-[(3-cholamidopropyl)dimethylammonio]-1-propanesulfonate, 5 mM DTT. From each brain, equal aliquots (25 μl) from the same homogenate were incubated at 37°C with recombinant active caspase-8 (0.1 unit/μl), and active caspase-3 (0.1 unit/μl; MBL, Watertown, MA). As a control, caspase-8 inhibitor z-IETD.fmk (200 μM, Enzyme Systems Products, Livermore, CA) was added before adding active caspase-8. After 4 h of incubation the samples were subjected to Western blotting (above) then probed for the 85-kDa PARP fragment by using an anti-cleaved PARP antibody (1:500, catalogue no. 9544, Cell Signaling Technology, Beverly, MA).

Statistical Analysis. Data are presented as mean ± SEM unless specified otherwise. Statistical comparisons were made by Student's *t* test or ANOVA as described (21, 22). $P < 0.05$ was considered statistically significant.
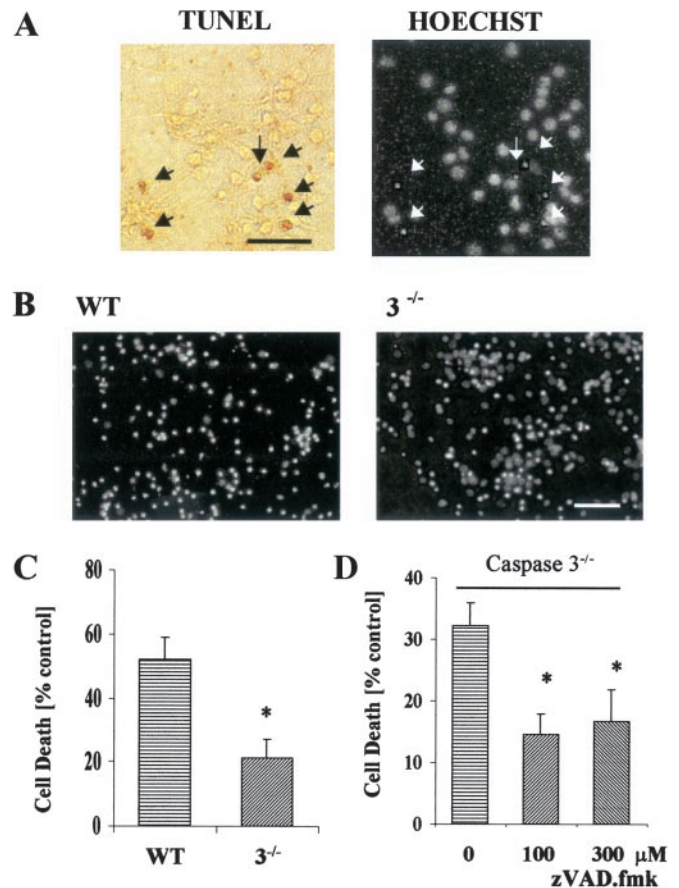
Results

Phenotypes of Adult Caspase-3$^{-/-}$ Mice. PCR was used to check the genotype of caspase-3$^{-/-}$ and WT mice (*in vivo* studies) or embryos used for cell cultures (*in vitro* studies). Caspase-3 proform on immunoblots was constitutively expressed in brains and neuronal cultures of WT littermates, but not in caspase-3$^{-/-}$ mice (not shown). The gross macroscopic features of adult caspase-3$^{-/-}$ forebrain, brainstem, and cerebellum did not differ significantly from WT littermates, contrasting to that described in neonatal caspase-3$^{-/-}$ mice bred on a different genetic background (129/Sv; refs. 11 and 12). The cerebral vasculature as visualized by carbon black perfusion (23) was normally developed. The circle of Willis was complete and the anastomosing vessels connecting anterior and middle cerebral arteries were equivalent between strains (not shown). Brain weights for the two adult strains were similar, although cortical gray matter was hypercellular in caspase-3$^{-/-}$ mice (Fig. 1). The density of neurons (NeuN-positive cells) determined by stereology was 26% greater in caspase-3$^{-/-}$ cortex (11.2 ± 2.2 × 10^6/mm^3 in mutant mice vs. 8.6 ± 0.8 × 10^6/mm^3 in WT littermates; $n = 5$ per group, $P < 0.05$). Cell morphology, however, did not differ
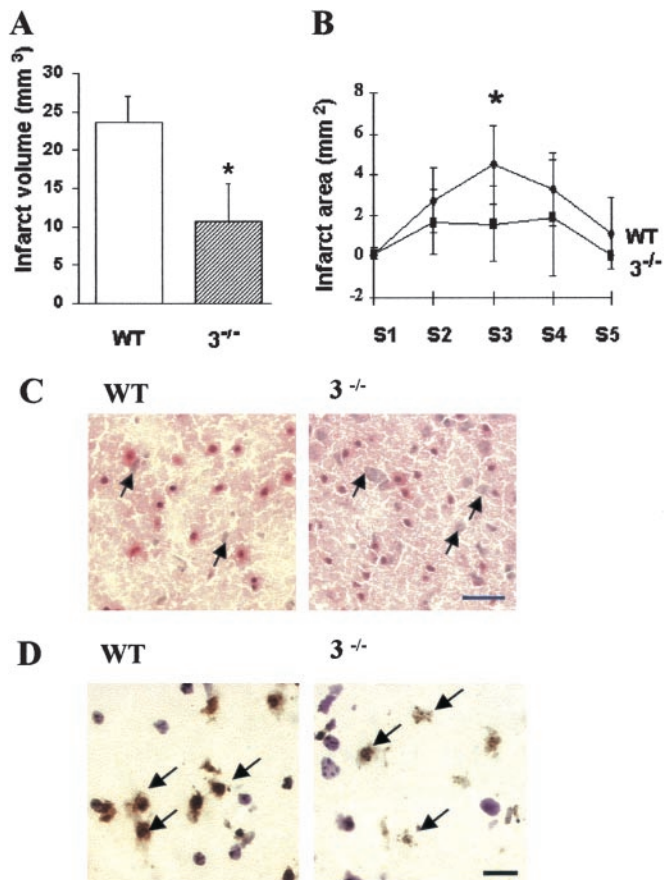
Fig. 2. Caspase-3$^{-/-}$ mice were resistant to ischemia induced by 2 h of distal MCAO and 48 h of reperfusion. (*A*) Infarct volume in caspase-3$^{-/-}$ mice (*n* = 7) was significantly smaller than in WT littermates (*n* = 9; *P* <0.05). (*B*) Infarct area was decreased in caspase-3$^{-/-}$ mice in section 3 (S3; *P* < 0.05). (*C*) Cortical injury was less severe in caspase-3$^{-/-}$ mice as compared with WT littermates with more normal appearing neurons (arrows) within the lesion (hematoxylin/eosin stain). (*D*) Fewer TUNEL-positive cells were present in ischemic caspase-3$^{-/-}$ cortex than in WT littermates. Many nuclei of TUNEL-positive cells exhibited condensed or irregular nuclear clumping (arrows; counterstained with cresyl violet). (Bars = 20 μm.)


Fig. 3. Cell death in neuronal cultures after 2 h of OGD and 22 h of reperfusion. (*A*) TUNEL-staining (black arrows) in WT corticoneuronal cultures colocalized with condensed nuclei (white arrows) of cells stained with Hoechst 33342. (*B* and *C*) Cell death was significantly less in caspase-3$^{-/-}$ cultured neurons than in WT cultures (*n* = 3 independent studies; *P* < 0.05). (*D*) Cell death was further attenuated in caspase-3$^{-/-}$-cultured neurons subjected to OGD and cotreated with zVAD.fmk (100 or 300 μM) in comparison with caspase-3$^{-/-}$-cultured neurons without zVAD.fmk treatment (*n* = 3, *P* < 0.02). No statistical difference occurred between zVAD.fmk (100 μM) and zVAD.fmk (300 μM) groups. (Bars = 50 μm.)

grossly between groups at the light microscopic level and the proportion of glial cells to neurons is approximately similar between wild type and mutants as reported (11, 12). Physiological parameters (*n* = 4 per group) including blood pressure, heart rate, cerebral blood flow, arterial pH, p_aCO_2, p_aO_2, and rectal temperature before and after MCAO did not differ between groups (not shown).

Neuroprotection in Caspase-3$^{-/-}$ Mice. In vivo *studies.* At 48 h after reperfusion, infarct size was significantly smaller (by 55%) in caspase-3$^{-/-}$ mice compared with their WT littermates. Mean values were 10.7 ± 4.9 in caspase-3$^{-/-}$ mice vs. 23.5 ± 3.6 in WT littermates (mm^3, *P* < 0.05; Fig. 2*A*). Infarct area from section 3 (S3) was significantly decreased (*P* < 0.05; Fig. 2*B*). Tissue injury was less severe in the caspase-3$^{-/-}$ mice with more normal appearing neurons throughout the lesion (Fig. 2*C*). *In situ* TUNEL staining was used to evaluate the contribution of DNA fragmentation to neuronal cell death after MCAO. The number of TUNEL-positive cells was dramatically decreased in caspase-3$^{-/-}$ cortex compared with WT littermates (Fig. 2*D*). The density of TUNEL-positive cells (per mm^3) in the sampled ischemic cortex was decreased by 36% in mutants (5.9 ± 1.9 × 10^6 in caspase-3$^{-/-}$ mice and 9.2 ± 5.2 × 10^6 in their WT

littermates; *P* < 0.05). The percentage of TUNEL-positive cells per total cells was also lower (0.53% vs. 1.1%).

In vitro *studies.* To assess whether caspase-3 deletion renders cultured neurons more resistant to cell death after OGD treatment, we counted cells with condensed or fragmented nuclei by using Hoechst stain from three WT cultures paired with three mutant cultures. More than 95% of Hoechst positive cells showing nuclear condensation or fragmentation were also TUNEL positive (Fig. 3*A*). We observed significantly less cell death (by 59%) in the caspase-3$^{-/-}$ neurons (52 ± 7% vs. 21 ± 6% control, *P* < 0.02; Fig. 3 *B* and *C*). When zVAD.fmk (100 or 300 μM) was added to mutant cultures, an additional protection (by ≈55%, *P* < 0.02 between nontreated group and zVAD-treated group at either concentration) was observed (Fig. 3*D*), suggesting involvement of caspase(s) other than caspase-3 in apoptotic cell death.

PARP Cleavage and Caspase Activation in Caspase-3$^{-/-}$ CNS. We detected the 85-kDa immunoreactive PARP cleavage fragment within nuclei of ischemic neurons *in situ* from both WT (not shown) and caspase-3$^{-/-}$ mice (Fig. 4*A*) and on immunoblots *in vivo* (Fig. 4*B*). Similarly, the 85-kDa PARP cleavage fragment was present in caspase-3$^{-/-}$ neurons after OGD (Fig. 4*C*), and
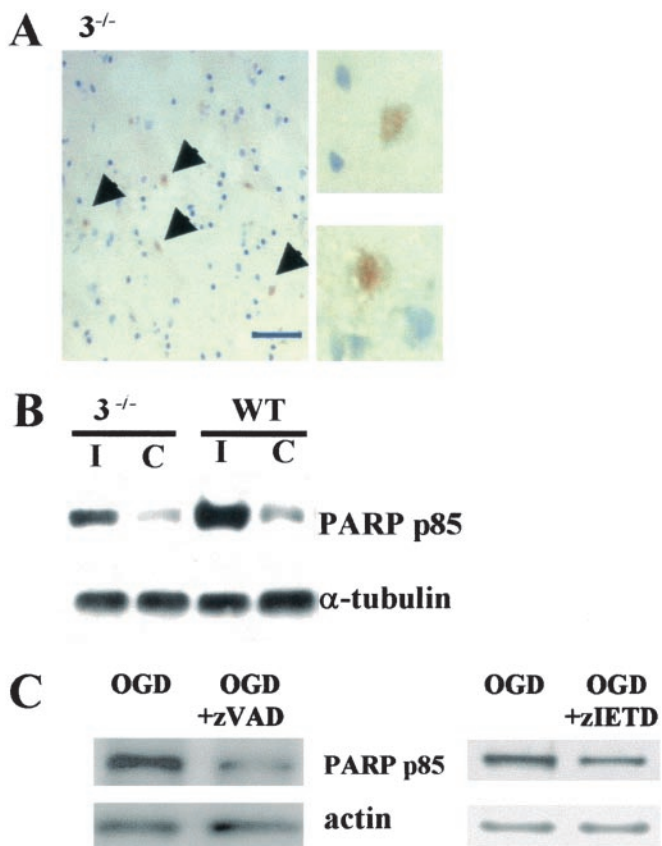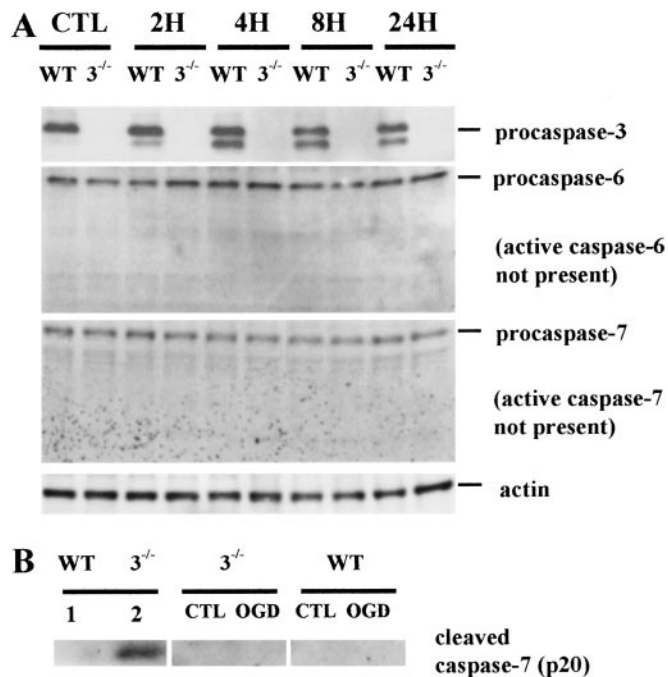
Fig. 4. Detection of cleavage products of PARP (85 kDa) in ischemic caspase-3$^{-/-}$ CNS *in vivo* and *in vitro*. (*A*) PARP p85 immunoreactivity was found within nuclei in ischemic cortex of caspase-3$^{-/-}$ mice subjected to 2 h of MCAO and 48 h of reperfusion (*Left*, low power; *Right*, high power). Counterstained with hematoxylin (striatal level). (*B*) PARP p85 was increased on the ischemic side (I) compared with contralateral cortex (C) in both groups after 2 h of MCAO and 48 h of reperfusion. (*C*) PARP p85 was suppressed by zVAD.fmk (100 μM) (*Left*) and zIETD (100 μM) (*Right*) in caspase-3$^{-/-}$ neuronal cultures subjected to 2 h of OGD and 22 h of reperfusion.

Fig. 5. Expression of caspase-3, -6, -7 at 2, 4, 8, and 24 h after OGD of neuronal cultures in WT and mutant mice. Antibodies were obtained from Cell Signaling Technology. (*A Top*) procaspase-3 (33 kDa) was detected in WT and not in caspase-3$^{-/-}$ cultures. ≈29 kDa was of unknown significance. (*Upper Middle*) Procaspase-6 (34 kDa) was constitutively present in both strains despite the absence of active caspase-6 p15. (*Lower Middle*) Procaspase-7 (35 kDa) was constitutively present in both strains despite the absence of active caspase-7 p20. (*B*) By using an antibody that recognizes only the active caspase-7 p20 (no. 9491, Cell Signaling Technology), the p20 fragment was detected in liver lysate of caspase-3$^{-/-}$ mice treated with anti-Fas antibody Jo-2 (lane 2) and but not in liver of WT mice treated with Jo-2 (lane 1) or in neuronal cultures of either strains subjected to 2 h of OGD and 22 h of reperfusion (*Center* and *Right*). CTL, control.

importantly, was suppressed by adding zVAD.fmk (100 μM; Fig. 4*C Left*), or zIETD.fmk (100 μM; Fig. 4*C Right*) during OGD and the reoxygenation period of caspase-3$^{-/-}$ cultures, implicating caspase(s) such as caspase-8 in PARP cleavage.

We next evaluated caspases-6, -7, and -8 as potential candidates for PARP cleavage in caspase-3$^{-/-}$ cells. Despite expression of the proforms of caspases-6 and -7, caspase-7 cleavage was not detected in ischemic cortical tissues of caspase-3$^{-/-}$ or WT mice (data not shown). Furthermore, cleavage of procaspase-6 or procaspase-7 was not detected after OGD, as well (Fig. 5*A*). The antibodies we used [caspase-6 Ab (no. 9762), cleaved caspase-7 Ab (no. 9491) from Cell Signaling Technology] did detect cleaved caspase-6 (15 kDa; data not shown) and cleaved caspase-7 fragment (19 kDa; Fig. 5*B*), respectively, in liver lysates of Jo2-treated caspase-3$^{-/-}$ mice as expected from a previous report (13).

PARP was cleaved by caspase-8 to yield an 85-kDa fragment as documented after activation of caspase-8 by granzyme B (24) or by death-inducing signaling complex (25). We therefore asked whether caspase-3 deficiency modified the expression and cleavage of caspase-8 and whether PARP cleavage was mediated by caspase-8 in the presence of caspase-3 deficiency. Procaspase-8 was constitutively expressed in cortical cells coexpressing NeuN within all cortical laminae of caspase-3$^{-/-}$ mice (Fig. 6*A*) and WT mice, and no apparent differences were detected between

the two groups. After ischemia, active caspase-8 (p18) was found in the cytoplasm of cells only within the ischemic zone and many were also TUNEL- positive (Fig. 6*A*). The density of caspase-8 p18 positive cells was not different between groups (data not shown). Twenty-four hours after ischemia, caspase-8 mRNA expression was up-regulated by about 2.5-fold in both groups with no significant differences (Fig. 6*C*). These data suggest that caspase-8 was processed similarly in brains of both mutant and WT mice after ischemia. To determine whether caspase-8 cleaves PARP in mutant and WT brain, we next treated brain homogenates with recombinant active caspase-8 (Fig. 6*D*). The 85-kDa PARP fragment was detected in caspase-3 null homogenates and was suppressed by cotreatment of active caspase-8 with a caspase-8 inhibitor, zIETD.fmk (200 μM; Fig. 6*D*). The 85-kDa PARP fragment did not appear after incubation of caspase-3$^{-/-}$ brain homogenates with recombinant active calpain, or cathepsin D (data not shown).

Discussion

Caspase-3, the most abundant caspase family member, is constitutively expressed as an inactive precursor in murine brain cells, chiefly neurons (6). The evidence for caspase-3 expression in adult rat brain seems less clear, at least in certain strains (26, 27). During ischemia, caspase-3 is cleaved and activated whereupon it degrades multiple substrates in cytoplasm and nucleus leading to cell death. Injury to brain and spinal cord activates caspases-3, -8, -9, -11 (6, 21, 28–31), and caspase inhibitors abrogate ischemic injury, especially during milder insults. Neu-

NEUROSCIENCE
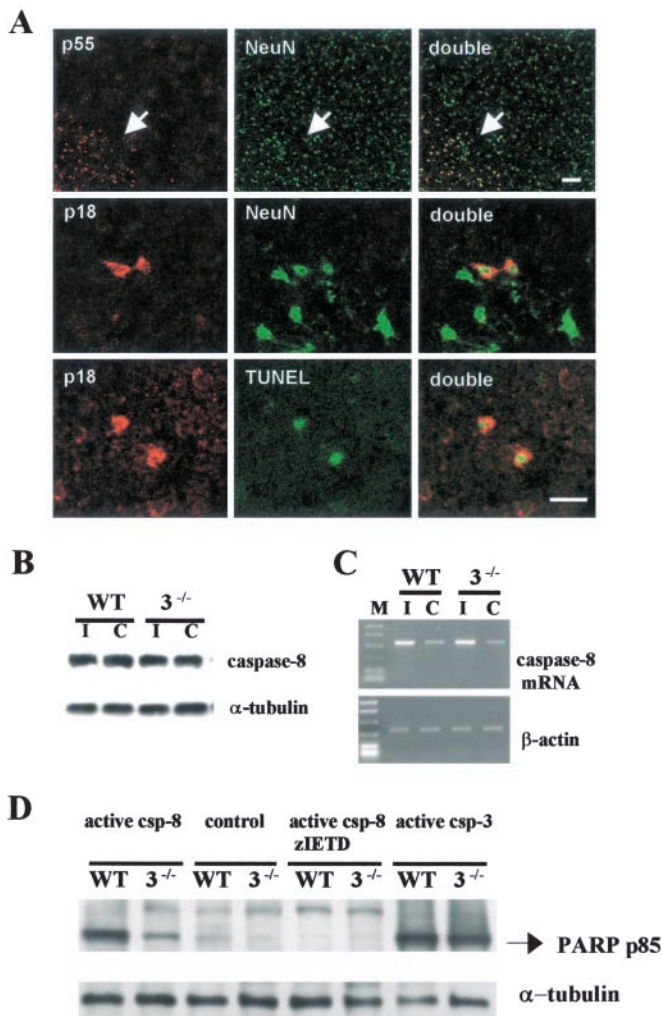
Fig. 6. Caspase-8 expression in frontal cortex of caspase-3$^{-/-}$ mice after 2 h of MCAO and 24 h of reperfusion. (*A Upper*) Procaspase-8 (p55; red) was constitutively expressed in NeuN-positive cells (green) and was enhanced in the outer margin of the ischemic territory (arrow). Caspase-8 p18 (*Middle*; red) was detected within the cytoplasm of neurons (green) and colocalized with TUNEL-positive cells (green; *Lower*). No apparent difference occurred in the number of caspase-8 p18 cells in caspase-3$^{-/-}$ and WT littermate mice after ischemia (not shown). Striatal level. (Bar = 20 μm.) (*B*) Caspase-8 p55 was detected in ischemic (I) and contralateral (C) cortex without apparent difference (by densitometry, not shown). (*C*) Agarose gel showing caspase-8 mRNA up-regulated in ischemic brain (I) (*Upper*). No differences between strains were determined (by densitometry, not shown). β-Actin was used as a housekeeping gene (*Lower*). (*D*) Recombinant active caspase-8 (0.1 unit/μl) cleaved endogenous PARP to the 85-kDa fragment in brain homogenates of both strains, and the effect was blocked by zIETD.fmk (200 μM). Recombinant active caspase-3 (0.1 unit/μl) was used for positive control.

roprotection in mice deficient in caspase-3 expression (Fig. 2*A*) is comparable with what we observed after i.c.v. administration of caspase inhibitors zDEVD.fmk or zVAD.fmk after MCA occlusion (32). In the *in vitro* OGD paradigm, caspase inhibitor zDEVD.fmk also abrogated neuronal death, and active caspase-3 was detected by immunoblots after OGD at 6 h and most strongly at 24 h (20). The studies above are limited, however, by the lack of selectivity of caspase inhibitors. Thus, to confirm directly the important role of caspase-3 in mediating ischemic neuronal death, we studied neurons cultured from caspase-3$^{-/-}$ mice.

The caspase-3$^{-/-}$ mice, bred from heterozygotes on a C57BL/6 mice background, seem to grow and develop like the

WT. Despite cortical hypercellularity (Fig. 1), the composition of CNS cell types including glial cells and neurons was similar to WT mice (11, 12). These mice were resistant to ischemic injury after 2 h of reversible distal MCA occlusion. The lesion, confined to cortical gray matter, was reduced by 55% from WT littermate controls. Blood flow distal to the occlusion and the anatomy of the circle of Willis did not differ between groups (carbon black perfusion). Consistent with the *in vivo* findings, caspase-3 mutant cultures showed less cell death ($\approx$59%) after OGD reflecting intrinsic resistance to injury and cell death in caspase-3$^{-/-}$ cells rather than to differences peculiar to organogenesis. Although the increased cell density in mutant brains could confound the observed neuroprotective effect *in vivo*, the resistance of caspase-3$^{-/-}$ murine brain may be understated because of differences in cell density between strains. A greater cell density imposes greater metabolic demands and blood flow requirements that exaggerate the mismatch that develops during ischemia between reduced blood flow (oxygen delivery) and increased tissue metabolism (oxygen demand). In other ischemic paradigms, this disparity causes more ischemic injury (33, 34). Taken together, the *in vivo* and *in vitro* data support a role for caspase-3 in neuronal death induced by ischemia and the significance of this caspase in rendering cells more resistant to ischemic stress.

Despite deletion of the caspase-3 gene, we observed features of apoptotic-like neuronal death both *in vivo* and *in vitro* [i.e., 85-kDa PARP cleavage fragment, TUNEL-positive cells, cells with condensed nuclei (Figs. 2*D* and 3*A*), plus protection with zVAD.fmk in caspase-3$^{-/-}$ cultures after OGD (Fig. 3*D*)]. Therefore, we explored the possibility that redundant caspases cleaved PARP in ischemic cell death. PARPs are nuclear enzymes that repair DNA and include many members from PARP-1 to -4, and VPARP (35). Cleavage of PARP (mainly PARP-1) to an 85-kDa fragment is preferentially mediated by caspase-3 (36, 37), although it can also be cleaved by other caspases less efficiently. In addition to caspase-3, other caspases that can cleave PARP to the 85-kDa fragment include caspase-7 (38, 39), caspase-6 (40), and caspase-8 (24, 25). Caspase-8 can cleave PARP-2, as reported (41).

Previously, compensatory activation of caspase-6 and -7 was reported for liver cells deficient in caspase-3 when treated with anti-Fas antibody, γ- and UV-irradiation (13). In our experiments, we focused on studying caspases-6, -7, and -8 in relation to the findings that PARP is cleaved in caspase-3$^{-/-}$ ischemic neurons *in vivo* and *in vitro*. However, cleavage of caspases-6 and -7 was not found in caspase-3$^{-/-}$ cultures subjected to OGD despite constitutive presence of both (Fig. 5*A*). The lack of caspases-6 and -7 activation in the nervous system unlike that in the liver of caspase-3$^{-/-}$ mice (Fig. 5*B*; ref. 13), suggests that stimulus-specific or organotypic differences may exist in caspase regulation, and that caspases-6 and -7 may not play a major role in mediating PARP cleavage in ischemic mutant neurons, despite their constitutive expression. In contrast, caspase-8 was activated in caspase-3$^{-/-}$ neurons after cerebral ischemia (Fig. 6*A*), and recombinant caspase-8 cleaved PARP to the 85-kDa fragment in caspase-3$^{-/-}$ brain homogenates (Fig. 6*D*). Furthermore, the appearance of the 85-kDa PARP fragment was partially suppressed after adding zIETD.fmk, a caspase-8 inhibitor, to mutant cultures subjected to OGD (Fig. 4*C*). Altogether, our data support a redundant role for caspase-8 in mediating PARP cleavage in caspase-3$^{-/-}$ neurons. In addition, the colocalization of active caspase-8 with TUNEL-positive neurons (Fig. 6*A*) suggests a role for caspase-8 in mediating cell death, as further supported by our preliminary results that zIETD.fmk (100 μM) also attenuated neuronal death in caspase-3$^{-/-}$ cultures (not shown).

Caspase-8-mediated cleavage of PARP was much less robust in caspase-3$^{-/-}$ brain extracts (Fig. 6*D*), as compared with WT

control, suggesting that in WT nervous tissue, PARP cleavage by caspase-8 is mainly mediated by caspase-3, perhaps from direct activation of caspase-3 by caspase-8 (42).

In summary, our findings indicate that genetic deletion of caspase-3 renders neurons resistant to mild ischemic injury *in vivo* and *in vitro*. Redundant mechanisms such as activation of caspase-8 promote cleavage of caspase substrates and persistent apoptotic-like cell death. Taken together, the data suggest that broad-spectrum caspase inhibition may afford more complete neuroprotection than single caspase targeting, and that PARP

cleavage after hypoxia and ischemia in caspase-3-deficient neurons is, in part, mediated by caspase-8.

1. Nicholson, D. W. & Thornberry, N. A. (1997) *Trends Biochem. Sci.* **22,** 299–306.
2. Cryns, V. & Yuan, J. (1998) *Genes Dev.* **12,** 1551–1570.
3. Nicholson, D. W. (1999) *Cell Death Differ.* **6,** 1028–1042.
4. Porter, A. G. & Jänicke, R. U. (1999) *Cell Death Differ.* **6,** 99–104.
5. Zheng, T. S., Hunot, S., Kuida, K. & Flavell, R. A. (1999) *Cell Death Differ.* **6,** 1043–1053.
6. Namura, S., Zhu, J., Fink, K., Endres, M., Srinivasan, A., Tomaselli, K. J., Yuan, J. & Moskowitz, M. A. (1998) *J. Neurosci.* **18,** 3659–3668.
7. Chen, J., Nagayama, T., Jin, K., Stetler, R. A., Zhu, R. L., Graham, S. H. & Simon, R. P. (1998) *J. Neurosci.* **18,** 4914–4928.
8. Hara, H., Friedlander, R. M., Gagliardini, V., Ayata, C., Fink, K., Huang, Z., Shimizu-Sasamata, M., Yuan, J. & Moskowitz, M. A. (1997) *Proc. Natl. Acad. Sci. USA* **94,** 2007–2012.
9. Fink, K., Zhu, J., Namura, S., Shimizu-Sasamata, M., Endres, M., Ma, J., Dalkara, T., Yuan, J. & Moskowitz, M. A. (1998) *J. Cereb. Blood Flow Metab.* **18,** 1071–1076.
10. Endres, M., Namura, S., Shimizu-Sasamata, M., Waeber, C., Zhang, L., Gomez-Isla, T., Hyman, B. T. & Moskowitz, M. A. (1998) *J. Cereb. Blood Flow Metab.* **18,** 238–247.
11. Kuida, K., Zheng, T. S., Na, S., Kuan, C., Yang, D., Karasuyama, H., Rakic, P. & Flavell, R. A. (1996) *Nature* **384,** 368–372.
12. Leonard, J. R., Klocke, B. J., D'Sa, C., Flavell, R. A. & Roth, K. A. (2002) *J. Neuropathol. Exp. Neurol.* **61,** 673–677.
13. Zheng, T. S., Hunot, S., Kuida, K., Momoi, T., Srinivasan, A., Nicholson, D. W., Lazebnik, Y. & Flavell, R. A. (2000) *Nat. Med.* **6,** 1241–1247.
14. Takahashi, K., Kamiya, K., Urase, K., Suga, M., Takizawa, T., Mori, H., Yoshikawa, Y., Ichimura, K., Kuida, K. & Momoi, T. (2001) *Brain Res.* **894,** 359–367.
15. Committee on Care and Use of Laboratory Animals (1985) *Guide for the Care and Use of Laboratory Animals* (Natl. Inst. of Health, Bethesda, MD), DHHS Publ. No. (NIH) 85–23.
16. Welsh, F. A., Sakamoto, T., McKee, A. E. & Sims, R. E. (1987) *J. Neurochem.* **49,** 846–851.
17. Huang, Z. H., Huang, P. L., Panahian, N., Dalkara, T., Fishman, M. C. & Moskowitz, M. A. (1994) *Science* **265,** 1883–1885.
18. Swanson, R. A. & Sharp, F. R. (1994) *J. Cereb. Blood Flow Metab.* **14,** 697–698.
19. Brewer, G. J. (1995) *J. Neurosci. Res.* **42,** 674–683.
20. Plesnila, N., Zinkel, S., Le, D. A., Amin-Hanjani, S., Wu, Y., Chiarugi, A., Thomas, S. S., Kohane, D. S. & Moskowitz, M. A. (2001) *Proc. Natl. Acad. Sci. USA* **98,** 15318–15323.
21. Matsushita, K., Wu, Y., Qiu, J., Lang-Lazdunski, L., Hirt, L., Waeber, C., Hyman, B. T., Yuan, J. & Moskowitz, M. A. (2000) *J. Neurosci.* **20,** 6879–6887.
22. West, M. & Gundersen, H. (1990) *J. Comp. Neurol.* **296,** 1–22.
23. Murakami, K., Kondo, T., Kawase, M., Li, Y., Sato, S., Chen, S. F. & Chan, P. H. (1998) *J. Neurosci.* **18,** 205–213.
24. Muzio, M., Chinnaiyan, A. M., Kischkel, F. C., O'Rourke, K., Shevchenko, A., Ni, J., Scaffidi, C., Bretz, J. D., Zhang, M., Gentz, R., *et al.* (1996) *Cell* **85,** 817–827.
25. Medema, J. P., Scaffidi, C., Krammer, P. H. & Peter, M. E. (1998) *J. Biol. Chem.* **273,** 3388–3393.
26. Hu, B. R., Liu, C. L., Ouyang, Y., Blomgren, K. & Siesjo, B. K. (2000) *J. Cereb. Blood Flow Metab.* **20,** 1294–1300.
27. Clark, R. S., Kochanek, P. M., Watkins, S. C., Chen, M., Dixon, C. E., Seidberg, N. A., Melick, J., Loeffert, J. E., Nathaniel, P. D., Jin, K. L. & Graham, S. H. (2000) *J. Neurochem.* **74,** 740–753.
28. Krajewski, S., Krajewska, M., Ellerby, L., Welsh, K., Xie, Z., Deveraux, Q., Salvesen, G. S., Bredesen, D. E., Rosenthal, R., Fiskum, G. & Reed, J. C. (1999) *Proc. Natl. Acad. Sci. USA* **96,** 5752–5757.
29. Springer, J. E., Azbill, R. D. & Knapp, P. E. (1999) *Nat. Med.* **5,** 943–946.
30. Vellier, J. J., Ellison, J. A., Kikly, K. K., Spera, P. A., Barone, F. C. & Feuerstein, G. Z. (1999) *J. Neurosci.* **19,** 5932–5941.
31. Kang, S. J., Wang, S., Hara, H., Peterson, E. P., Namura, S., Amin-Hanjani, S., Huang, Z., Srinivasan, A., Tomaselli, K. J., Thornberry, N. A., *et al.* (2000) *J. Cell Biol.* **149,** 613–622.
32. Hara, H., Waeber, C., Huang, P. L., Fujii, M., Fishman, M. C. & Moskowitz, M. A. (1996) *Neuroscience* **75,** 881–890.
33. Back, T., Hoehn, M., Mies, G., Busch, E., Schmitz, B., Kohno, K. & Hossmann, K. A. (2000) *Ann. Neurol.* **47,** 485–492.
34. Huh, P. W., Belayev, L., Zhao, W., Koch, S., Busto, R. & Ginsberg, M. D. (2000) *J. Neurosurg.* **92,** 91–99.
35. Smith, S. (2001) *Trends Biochem. Sci.* **26,** 174–179.
36. Nicholson, D. W., Ali, A., Thornberry, N. A., Vaillancourt, J. P., Ding, C. K., Gallant, M., Gareau, Y., Griffin, P. R., Labelle, M., Lazebnik, Y. A., *et al.* (1995) *Nature* **376,** 37–43.
37. Tewari, M., Quan, L. T., O'Rourke, K., Desnoyers, S., Zeng, Z., Beidler, R., Poirier, G. G., Salvesen, G. S. & Dixit, V. M. (1995) *Cell* **81,** 801–809.
38. Lippke, J. A., Gu, Y., Sarnecki, C., Caron, P. R. & Su, M. S. (1996) *J. Biol. Chem.* **271,** 1825–1828.
39. Germain, M., Affar, E. B., D'Amours, D. & Dixit, V. M. (1999) *J. Biol. Chem.* **274,** 28379–28384.
40. Orth, K., Chinnaiyan, A. M., Garg, M., Froelich, C. J. & Dixit, V. M. (1996) *J. Biol. Chem.* **271,** 16443–16446.
41. Benchoua, A., Couriaud, C., Guégan, C., Tartier, L., Couvert, P., Friocourt, G., Chelly, J., Ménissier-de Murcia, J. & Onténiente, B. (2002) *J. Biol. Chem.* **277,** 34217–34222.
42. Scaffidi, C., Fulda, S., Srinivasan, A., Friesen, C., Li, F., Tomaselli, K. J., Debatin, K. M., Krammer, P. H. & Peter, M. E. (1998) *EMBO J.* **17,** 1675–1687.

NEUROSCIENCE